Out of resonance infrared fluorescence of SF6, 1 2CF3I, 1 3CF3I in quasicontinuum states. I

C. Angelie

Citation: The Journal of Chemical Physics **96**, 8072 (1992); doi: 10.1063/1.462359
View online: http://dx.doi.org/10.1063/1.462359
View Table of Contents: http://scitation.aip.org/content/aip/journal/jcp/96/11?ver=pdfcov
Published by the AIP Publishing

Out of resonance infrared fluorescence of SF_6, $^{12}CF_3I$, $^{13}CF_3I$ in quasicontinuum states. I

C. Angelie
CEA– CEN Saclay–DSM–DRECAM–SPAM, 91191 GIF-Sur-Yvette Cedex, France

(Received 15 November 1991; accepted 26 February 1992)

IR fluorescence of SF_6 has been monitored in the spectral range 700–1300 cm^{-1} with a high sensitivity device, after IR multiphoton excitation at several vibrational energies up to 17 000 cm^{-1}. Preliminary results have also been obtained for $^{12}CF_3I$ and $^{13}CF_3I$. The sensitivity achieved allows us to focus on the out of resonance fluorescence which turns out to be directly proportional to the local intramolecular couplings represented by the parameter $\gamma(E \rightarrow E') = \pi\rho(E')|V(E \rightarrow E')|^2$. The method is partly free from an inhomogeneous contribution and the result can be compared to the Lorentzian model of intramolecular redistribution. It is shown that the $\gamma(E \rightarrow E')$ parameter exhibits a hierarchy of structures, the strongest couplings leading mainly to a perturbative redistribution, while the weakest couplings are responsible for the dissipative redistribution. The homogeneous dissipative part γ_d appears to be smaller than 1–1.5 cm^{-1}.

I. INTRODUCTION

This paper is the first of a series of four in which the spectral characteristics of SF_6, excited in its vibrational quasicontinuum (QC), will serve as a basis to point out a general framework capable of depicting the main features of intramolecular vibrational relaxation (IVR) of highly excited states, explored so far for a great variety of molecules.

Since the first study of IR multiphoton absorption (IRMPA), in 1971, the concept of rovibrational QC was introduced to explain how anharmonic shifts of several tens of cm^{-1} could be overcome by intramolecular mixing between zero order separable mode states.[1] For several years the QC was qualitatively understood as consisting of states able to absorb or emit in a broad spectral range, e.g., over several hundreds of cm^{-1}. In 1978, Bott performed a fluorescence spectrum of SF_6 excited at a vibrational energy $E_v \sim 14\,000$ cm^{-1} by a shock wave device.[2] The result gave a decisive blow to the previous point of view: The total spectral width of the ν_3 frequency structure, including homogeneous and inhomogeneous contributions, does not exceed 40 cm^{-1}. Thus spectral structures survive in the QC.

The presence of such spectral structures are often considered as an indication that there is no IVR in the molecule. This is not correct, as can be easily understood in the framework of the Bixon and Jortner (BJ) model of IVR:[3] IVR is described by constant couplings v between a doorway state and a bath of prediagonalized states having a density ρ. This leads to Lorentzian spectral shapes with half-width parameter $\gamma = \pi\rho v^2$, and to an exponential relaxation of the doorway state vs time, with a time constant decay τ_{IVR}, such that

$$2\gamma\tau_{IVR} = 5.3 \text{ cm}^{-1} \text{ ps}. \quad (1)$$

Thus a narrow structure of, e.g., 1 cm^{-1} is fully compatible with a statistical redistribution over a great number of states, since ρ can be as high as 10^{10}–10^{20} states/cm^{-1} in the QC.

Bott's spectrum gave only an upper bound to the homogeneous linewidth $\Delta\nu_h = 2\gamma$, since the observed spectrum was congested and spread out by the inhomogeneous contribution $\Delta\nu_{inh}$ due to the presence of a broad thermal distribution of initial states. Inhomogeneous contributions are the poison of spectral experiments exploring QC states.

In 1983, we used the BJ model to describe QC transition matrix elements of SF_6 and to analyze both IR fluorescence and IRMPA data. γ was considered as the adjustable parameter.[4] The first conclusion was that in Bott's spectrum, the inhomogeneous contribution explains the dominant part of the observed linewidth, so that $\Delta\nu_h \ll 40$ cm^{-1}. The second conclusion was that IRMPA data allow the extraction of a single $\gamma(E_v)$ parameter, depending weakly on the exact vibrational distribution formed by IRMPA. The resulting function grows linearly from a value $\gamma \sim 1$ cm^{-1} at the QC threshold ($E_v \sim 4000$ cm^{-1}) up to a value $\gamma \sim 12$ cm^{-1} near the dissociation threshold ($E_d \sim 32\,000$ cm^{-1}). Under the conditions of Bott's spectrum, γ is predicted to be ~ 5 cm^{-1}.

Although indirect and model dependent, this work is up to now the single one in which the SF_6 homogeneous linewidth has been estimated. There is, however, another approach which has given information about the SF_6 IVR: temporal picosecond studies.[5] Strong IVR manifestations appear for pulses of duration $\tau_L \sim 20$ ps, but the absorption of many photons and the broad distribution monitored make the extraction of τ_{IVR} difficult.

For molecules other than SF_6, several techniques have been developed in the past ten years, which have given greatly improved information about highly excited states. We have published elsewhere a review of the main work in this field[6] and will quote only a few typical results. $(CF_3)_3CI$ (Ref. 7) and CF_3I (Ref. 8) have been monitored near their dissociation threshold, with a technique reducing the inhomogeneous contribution to less than 3 cm^{-1}. The spectra appear strongly structured with peaks having a homogeneous linewidth of a few cm^{-1}. The spectroscopy of C–H benzene overtones up to 8800 cm^{-1} has also demonstrated spectral structure widths not exceeding 2 cm^{-1}. The problem of the inhomogeneous broadening is, however, not completely suppressed. On the other hand, temporal experiments have demonstrated IVR decay times beginning in the

 0021-9606/92/118072-14$06.00

range of 100 ps at the QC threshold and decreasing to around 20–2 ps at higher energies,[9] which gives $\Delta\nu_h \sim 0.25$–2.5 cm^{-1} according to (1). Thus QC states are highly structured with homogeneous widths probably lying in the previous range 0.25–2.5 cm^{-1}.

In this work, IR fluorescence experiments have been performed on SF_6 excited by IRMPA in its QC. These experiments are comparable to Bott's spectrum. The first difference is that the rotational temperature is weakly enhanced by IRMPA.[4] The second and much more important difference lies in the sensitivity of the detection which makes it possible to measure fluorescence intensities down to 10^{-3} of the spectrum maximum and therefore to analyze the out-of-resonance fluorescence, far from the ν_3 peak, continuously from 700 to 1300 cm^{-1}. As will be explained in the next section, this out of resonance fluorescence is essentially proportional to the parameter $\langle \gamma(E \to E + h\nu) \rangle$, i.e., the average of $\pi\rho|V|^2$ over the inhomogeneous distribution. This is information much more interesting than an upper limit $\gamma \ll \Delta\nu_{\text{inh}}$, as in Bott's spectrum, since it is directly related to the distribution of the intramolecular couplings $|V_{ij}|^2$.

This paper is mainly devoted to the experimental methods and results. The consequences will be analyzed in detail in the three subsequent papers, leading to a general framework able to reproduce all the essential trends of IVR, whatever be the molecule.

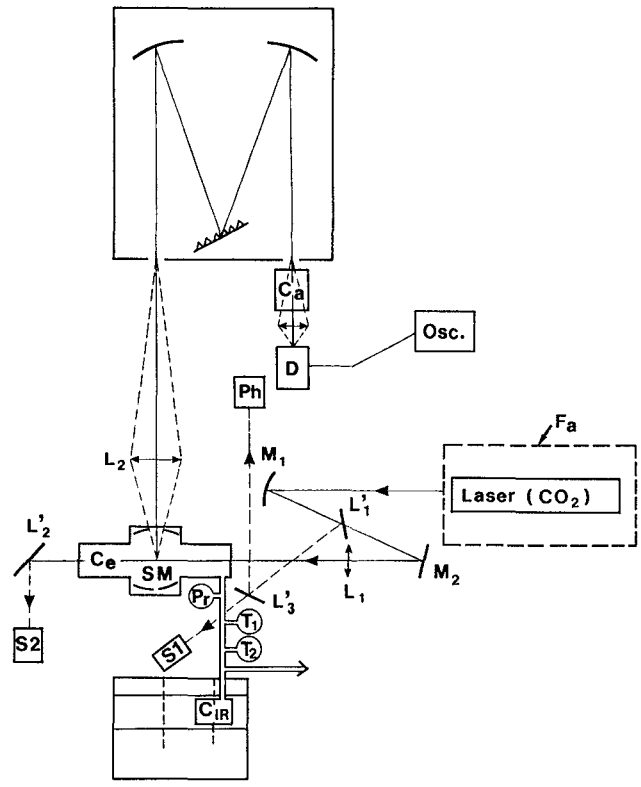

FIG. 1. Experimental device for fluorescence collection.

II. EXPERIMENTAL METHOD

A. Experimental device

The experimental device is represented in Fig. 1. The pulsed CO_2 laser is a model CGE CT 45C used at a repetition rate of 1 Hz. The pulse energy is 1 J without nitrogen tail and up to 4 J with nitrogen. The intensity fluctuations shot-to-shot are $\pm$ 6%. The temporal width is 200 ns with a 2 μs tail in presence of nitrogen. The laser is contained in a Faraday shielding F_a. The beam enters the cell C_e with a quasiparallel geometry, the diameter being 13 mm at the 1/e point. A photondrag detector Ph triggers the oscilloscope Osc and the energy absorbed is measured with a ratiometer RJ 7200 Laser Precision Corp. (probes $S1$, $S2$). The experimental cell is connected with a pressure sensor Pr Datametrics 1500, several nitrogen traps ($T_1, T_2, \cdots$) and an IR spectrometer Perkin–Elmer 281 (C_{IR} cell) which allows us to monitor the dissociation at the end of the experiment.

Inside the cell C_e, the fluorescence is collected by a system of four mirrors SM, as in a Welsh cell,[10] but in a different configuration. Figure 2(a) indicates the centers of the four mirrors, while the optical path of a half-beam is represented in Fig. 2(b). The fluorescence emitted through the transverse exit window is potentially multiplied by 10: five conical emissions towards the mirrors 1 and 2, and five parallel emissions across the laser beam. Practically, the geometrical distortions limit the gain to 6.5. Through the lens L_2 ($F_2 = 250$ mm, enlargement X2), the emitted fluorescence enters a monochromator Jobin–Yvon HR 1000 equipped with a 140×110 mm^2 grating. The entrance slit has a width l_M, generally fixed at its maximum $\bar{l}_M = 3$ mm, giving a resolution $\Delta\nu_r = 3.5$ cm^{-1}.

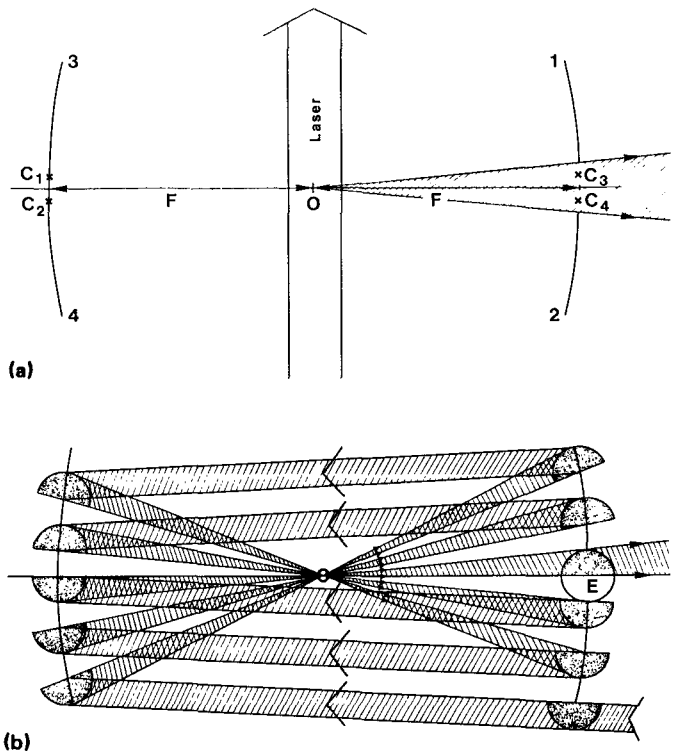

FIG. 2. System of mirrors SM: (a) General configuration. C_i: center of the mirror i. (b) Optical path of a half-beam of emitted fluorescence inside SM towards the exit window. The laser beam is as in Fig. 2(a).

After the exit slit, the fluorescence crosses an absorbing cell C_a containing a mixture SF_6/air of 6 Torrs/500 Torrs. The air broadens the SF_6 rotational transitions and gives a continuous absorption in the ν_3 range 940–951 cm^{-1}. The purpose of the cell C_a is to stop all parasitic reflections of the laser beam that would be fatal for the detector and its amplifier. In fact, reflections of the 10^7 W laser beam can reach values $\sim 10^2$ W. The cell C_a has an optical isolation of 10^{10}, so that the detector receives only parasitic intensities $\sim 10^{-8}$ W, i.e., the noise value. Moreover, this slight effect occurs only during the laser pulse. The blind window from 940 to 951 cm^{-1} is a weakness of the experiment since it concerns the ν_3 zone. However, this is not very important because the maximum ν_m is shifted by anharmonicity out of this range and the missing part can be approximately interpolated to give accurately the spectrum area. Moreover, we are mainly interested by out-of-resonance intensities.

The filtered fluorescence is focused by a lens L_3 of focal $F_3 = 20$ mm (enlargement X10) on the active area 1×1 mm^2 of the HgCdTe detector Infrared Ass. Inc. HCT 70, cooled by liquid nitrogen. The choice of L_3 allows to collect all the monochromator aperture and the maximum part of the irradiated gas height. On the other hand, it is the slit width which limits the transverse collected volume for $l_M \leqslant 10$ mm. The resulting collected fluorescence corresponds to a volume formed by the full laser beam diameter (13 mm), a height of 5 mm limited by the detector area, a width 1.5 mm limited by the monochromator slit, and a solid angle 3.5×10^{-2} Ster, multiplied by the gain of the system of mirrors, 6.5.

The HgCdTe detector has a response time $\tau = 200$ ns, a parameter $D^* = 1.4\ 10^{10}\,cm\,Hz^{1/2}/W$ at 77 K, corresponding to a noise intensity of 9 nW. The maximum responsivity is at 10.6 μm. The signal is multiplied by an amplifier PPA 15 (gain 10^3) and directed either to an oscilloscope Tektronix 7603/7D20, or to a data system Tektronix R7912, monitor 632, controller CP4165-CP115.

The signal obtained for each wavelength λ, defined by the monochromator, is $S(\lambda,t)$, in mV. The temporal dependence shows the SF_6 excitation by the laser pulse during 3 μs, and after 6 μs, an exponential decay corresponding to the V–T intermolecular transfer. The excited spectra have been recorded at $+6$ μs, before the decay but after an advanced vibrational thermalization. The experiments have been performed at a pressure $P = 0.370$ Torr, corresponding to a hard-sphere collisional time of about 300 ns. As resonant V–V transfer in the QC are faster than the hard-sphere rate,[5(a),11] V–V thermalization can be assumed.

B. Analysis of the data

1. Extraction of the oscillator strength $dF_c/d\nu$

The experimental data is $S(\lambda,t_1)$ obtained at the delay $+6$ μs, for a pulse energy W which presents shot-to-shot fluctuations $\sim \pm 6\%$. Far from the ν_3 peak, the signal can be of the same magnitude as the detector noise, ± 5 mV. Then, $S(\lambda)$ is averaged over ΔN_0 pulses ($\Delta N_0 \sim 20$). A temporal average is made over $[t - \Delta T, t + \Delta T]$, with $\Delta T = 1$ μs. The signal is also normalized to a given energy W_0 through a linear correction

$$S(\lambda,W_0) = \left[1 + K(\lambda)\frac{W_0 - \langle W\rangle}{W_0}\right] S(\lambda,\langle W\rangle).$$

$K(\lambda)$ is the exponent fitting the dependence of S on W, and belongs typically to the range [0.7–1.5]. The signal resulting from these corrections has an uncertainty $1\sigma = \pm 0.6$ mV.

In some experiments around the ν_3 maximum, the monochromator slit was reduced, so that the signal must also be normalized, linearly, to the value $\bar{l}_M = 3$ mm. The correction factor was determined experimentally. The next correction concerns the external optical device responsivity $C_f(\lambda)$ (lens, monochromator, absorbing cell C_a, detector). This responsivity has been measured using a blackbody heated at 170 °C, which emits the intensity $B(\lambda,T)$ (in $W/nm \times cm^2 \times Ster$). Then, the detector response is given by

$$S = C_f(\lambda)[B(\lambda,T) - B(\lambda,T_0)],$$

where T_0 is the laboratory temperature. Except the absorbing cell range 940–951 cm^{-1}, the maximum responsivity is reached between 900–1100 cm^{-1} and declines to 20% at 700 and 1300 cm^{-1}. Then, the function $S(\lambda,W_0)/C_f(\lambda)$ gives the net fluorescence $dI_e/d\lambda$ emitted at the exit window of the experimental cell C_e (in a unit proportional to $W/nm \times cm^2 \times Ster$).

It must be mentioned that SF_6 dissociates slowly during the experiment. The IR spectrometer allows us to measure the final dissociation, which is always kept below 20%, and to compute the density after the Nth pulse $n(N) = n(0)e^{-\delta N}$. This value is used in further corrections as indicated below. No correction has been made for the products appearing in the cell ($SF_4 \cdots$) because they are not significantly excited at $+6$ μs, the collisional V–V thermalizaton being in the range of a few tens of μs for nonresonant transfers. However, it is better to correct the results for the $^{34}SF_6$ contribution since it is present in a quantity of 4%.

It is useful to express the quantities vs the frequency and in terms of oscillator strength $dF/d\nu$. The apparent oscillator strength at the cell exit is, therefore,

$$\frac{dF_e}{d\nu} = \frac{1}{\nu^3}\frac{dI_e}{d\nu} \tag{2a}$$

with

$$\frac{dI_e}{d\nu} = \frac{1}{\nu^2}\frac{dI_e}{d\lambda}. \tag{2b}$$

This apparent oscillator strength $dF_e/d\nu$ must be related to the corrected one, $dF_c/d\nu$, corresponding to the direct emission of a small volume of SF_6 molecules thermalized at a temperature T characteristic of the irradiated volume, at $t = +6$ μs. Several facts must be taken into account. First, the irradiated volume is modeled by a constant temperature T_1 within a radius r_1 and the laboratory temperature T_0 outside. Second, the signal emitted by a small volume travels through the system of mirrors and can be reabsorbed, either in the cold gas volume, or, mainly in the irradiated volume. While the reabsorption is negligible in the wings of the ν_3 mode, it can reach 25% around the maximum. Third, the detector is sensitive only to the intensity variation, and the undetected blackbody emission $B(\nu,T_0)$ must be taken into

account. The relation between $dF_e/d\nu$ and $dF_c/d\nu$ is stated in Appendix A.

It deserves to be mentioned that for $t \geqslant 15\ \mu$s, the V–T transfer heats the gas translations and produces an adiabatic expansion which modifies both T_1, n_1, and r_1, needing further corrections which have been studied elsewhere.[12] Here, at $t = +6\ \mu$s, these corrections are irrelevant.

2. Extraction of the local parameter $\gamma(E \rightarrow E')$

The measured oscillator strength $dF_c/d\nu$ results from an integration of the homogeneous dipole transition matrix elements, i.e., matrix elements for a molecule in a given (E,J) state, over the inhomogeneous distribution $P(E,J)$. The fundamental parameters we need are those of the homogeneous expressions. We have thus to use an expression which can be derived in the general model of a prepared (doorway) state $|s\rangle$ coupled to a dense set of prediagonalized states $|\bar{n}\rangle$ by matrix coupling elements V_{sn}. This model has a long history and has been studied under various particular assumptions.[3,4,12–14] The published results are sufficient for the present purpose but the model will be reinvestigated in the subsequent papers III and IV, relaxing almost all restrictions. In what follows, we give the basis of the out of resonance fluorescence method. Details and refinements are given in Appendix B.

In the previous frame, a transition operator d prepares the doorway state from an exact eigenstate

$$|s\rangle = d\,|E\rangle. \tag{3}$$

The transition matrix elements obey formally a Lorentzian expression

$$|\langle E\,|d\,|E'\rangle|^2 = \|d\,|E\rangle\|^2 L(E \rightarrow E') \tag{4a}$$

with

$$L(E \rightarrow E') = \frac{1}{\pi} \frac{\gamma(E \rightarrow E')}{[E' - E_s - F(E')]^2 + D^2(E \rightarrow E')}. \tag{4b}$$

In an optical transition

$$E' = E + h\nu. \tag{4c}$$

The formal appearance of a Lorentzian function must not mask the fact that the different parameters γ, E_s, F, and D can depend on E and E'. These parameters are made explicit in Appendix B 1. γ is the half-width of the Lorentzian function and is related to the density of states ρ and the effective coupling V_e [Eq. (B1a)] by

$$\gamma = \pi\rho(E')|V_e(E \rightarrow E')|^2. \tag{4d}$$

E_s is the average energy of the doorway state $|s\rangle$ and can be expressed, for a vibrational transition, by an anharmonically shifted frequency

$$E_s - E = h\nu_s(E_v) = h\nu_s(0) - a_s E_v, \tag{4e}$$

where a_s is the anharmonic coefficient. F is an energy shift of the resonance, generally small, and $D = \gamma$ in the most common situation, although corrections or reinterpretations of D are necessary in several cases (see Appendix B 1 and B 2).

As will be analyzed in papers III and IV, the main problem of the formal expression (4b) is due to the possible strong variations of the function $|V_e(E \rightarrow E')|^2$, vs E', strong variations due to the existence of multiple secondary resonances. In this case, F and D also have strong variations and the Lorentzian shape is no longer relevant. Each resonance α must be treated by a Lorentzian function L_α with a weight $P_\alpha(E_v)$. However, if these secondary resonances are perturbative ($P_\alpha \ll 1$), it can be shown that they can be treated as isolated peaks for γ [numerator of Eq. (4b)], at appropriate location E_α, F, and D having only regular variations,

$$\Delta\gamma_\alpha = \pi|V_{e\alpha}|^2 L_\alpha(E' - E_\alpha), \tag{5}$$

where $V_{e\alpha}$ and E_α depend on E (see Appendix B 2). L_α can be treated as a δ distribution. This gives a unified way to treat the redistribution of the oscillator strength, whatever be the situation: i.e., flat or structured distribution of couplings. The important remark is that the Lorentzian denominator varies regularly and that, out of resonance, it is weakly dependent on γ, its zero order approximation being $[h\nu - (E_s - E)]^2$. Such a function L with a regular denominator will be called a "quasi-Lorentzian" function.

The resulting oscillator strength can be written

$$\frac{dF_c}{d\nu} = \frac{8\pi^2}{3}\frac{h^2}{c^2} A_3 \frac{\nu}{\nu_m} \exp\left[-h\frac{\nu - \nu_m}{kT_1}\right] I(\nu) \tag{6a}$$

with

$$I(\nu) = \sum_\alpha \int dE_v dE_J P_v(E_v) P_J(E_J) \times \bar{v}_3(E_v) P_\alpha(E_v) L_\alpha(E_v, J, \nu). \tag{6b}$$

A_3 is the integrated absorption cross section of the ν_3 mode, known from the cold gas absorption spectrum, which does not depend on the particular rovibrational distribution. ν_m is the frequency of the spectrum maximum. T_1 is the vibrational temperature of the irradiated zone. The vibrational distribution P_v is thermal at a temperature T_1, while P_R is also thermal but at a temperature T_0, since it has been justified in Ref. 4 that IRMPA produces a weak rotational heating. $\bar{v}_3(E_v)$ is the average number of quanta in one coordinate of the ν_3 mode for a molecule at a vibrational energy E_v. It can be computed assuming an intramolecular thermal distribution between the modes (see Ref. 4).

In (6b), intense resonances must be treated separately, while perturbative resonances are grouped in a single function L with a regular denominator, as indicated above. Rotations are taken into account in a simplified way, as in Ref. 4 (see Appendix B 1). The relation (6) is used through the ratio

$$\frac{dF_c}{d\nu}(\nu) \Big/ \frac{dF_c}{d\nu}(\nu_m) = X(\nu),$$

as explained in Appendix A [Eqs. (A7)].

The out-of-resonance fluorescence can be analyzed in the following way. $P_v(E_v)$ is a function having its maximum values in a range $R_p = [\langle E_v\rangle - \Delta_v, \langle E_v\rangle + \Delta_v]$ and exponentially decreasing out of this range. The quasi-Lorentzian function L has its maximum values in a range

$$R_L = \left[\bar{E}_v - \frac{\gamma}{a_s}, \bar{E}_v + \frac{\gamma}{a_s}\right],$$

where

$$\nu = \nu_s(\overline{E}_v). \tag{7}$$

Then the integrand of $I(\nu)$ has two well-separated maxima when the condition of out-of-resonance is fulfilled,

$$|h\nu - h\nu_s(\langle E_v\rangle)| \gg \gamma, a_s\Delta_v. \tag{8}$$

There are, therefore, two contributions to the integral I. The first, due to the range R_P, can be approximated by

$$I_1(\nu) \sim \frac{1}{\pi}\frac{\langle\overline{v}_3\rangle_P}{(h\Delta\nu)^2}\langle\gamma(\nu)\rangle_P \tag{9a}$$

with

$$\Delta\nu = \nu - \nu_s(\langle E_v\rangle), \tag{9b}$$

$$\langle\gamma(\nu)\rangle_P = \int dE_v P_v(E_v)\gamma(E_v, E_v + h\nu). \tag{9c}$$

The variation of the Lorentzian denominator is neglected over R_P, so that the approximation is not accurate. Better approximations are detailed in Appendix B 3 but formulas (9) give the main characteristics of $I_1(\nu)$: $I_1(\nu)$ decreases slowly with ν as $1/\Delta\nu^2$, and is proportional to an average of γ over the distribution P_v.

The second contribution, over the range R_L, can be approximated by

$$I_2(\nu) \sim \overline{v}_3(\overline{E}_v)P_v(\overline{E}_v). \tag{10}$$

Here, the variation of P_v over R_L is neglected. The most important point is that $P_v(\overline{E}_v)$ tends to zero exponentially with $|\Delta\nu|$ (or is strictly zero for $\overline{E}_v < 0$) so that $I_2 \ll I_1$ out of resonance. $I_2(\nu)$ corresponds to the fluorescence for a nonredistributed line ($\gamma \to 0$) and can be computed separately, so that the correction I_2 can be made and the condition $I_2 \ll I$ checked.

The previous procedure allows us to extract the information $\langle\gamma(\nu)\rangle_P$ which, although being an average, is not limited by the condition $\gamma \gtrsim a_s\Delta_v$, as in the case of the fluorescence around resonance.

When the spectrum $I_1(\nu)\Delta\nu^2$ presents local peaks, they must be interpreted as due to secondary resonances α. It can be checked, in this case, that the integration of $\Delta I_\alpha(\nu)\Delta\nu^2$ gives the effective coupling $|V_{e\alpha}|^2$ (Appendix B 4),

$$\int d\nu\, \Delta I_\alpha(\nu) h^2 \Delta\nu^2 \sim \langle\overline{v}_3\rangle\langle|V_{e\alpha}|^2\rangle_P. \tag{11}$$

Then, according to the case, the out-of-resonance fluorescence method gives the values $\langle\gamma(\nu)\rangle_P$ or $\langle|V_{e\alpha}|^2\rangle_P$.

III. EXPERIMENTAL RESULTS

A. SF_6

The absorption spectrum $\sigma_{\alpha 0}(\nu)$ of the cold SF_6 (laboratory temperature T_0) has been recorded at 0.37 Torr around the ν_3 peak (scale X1), and at 37 Torr out of resonance (scale X100) in view of comparing the redistribution of the oscillator strength in the discrete levels and in the QC. Moreover, this allows the computation of the correction due to the reabsorption in the cold zone (Eq. A9), which is in fact negligible out of resonance. The resulting spectrum is given in Fig. 3. The central part, corresponding to the ν_3 peak (948 cm^{-1}), has an integrated cross section[15] $A_3 = 1.765\ 10^{-16}$ cm. The only noticeable resonances and

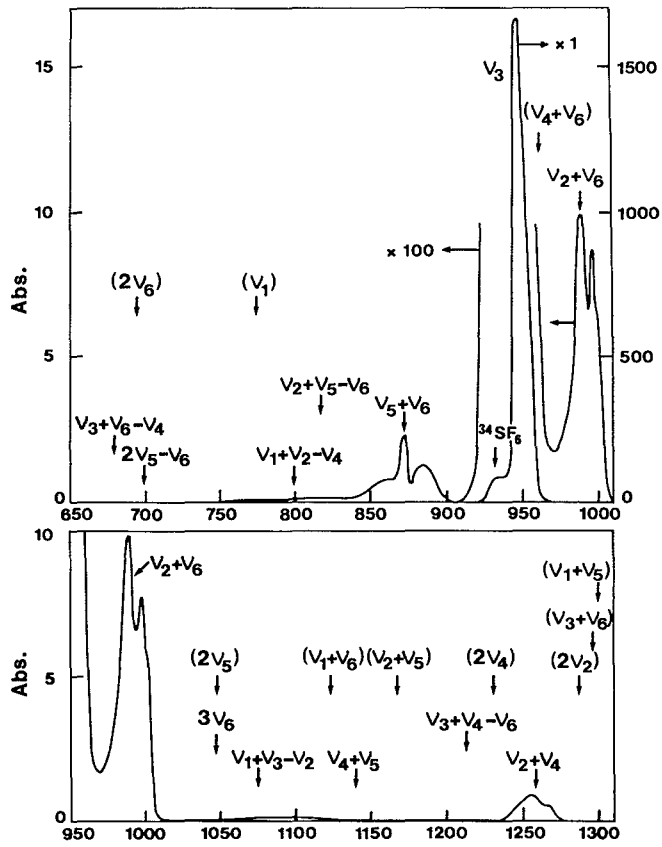

FIG. 3. Absorption spectrum of SF_6 at the laboratory temperature and low intensity. Scale X1: 0.37 Torr. Scale X100: 37 Torr.

their effective couplings $|V_e|$, computed according to Eqs. B5, are $\nu_5+\nu_6$ (872 cm^{-1}, $V_e = 4.2$ cm^{-1}), $\nu_2+\nu_6$ (991 cm^{-1}, $V_e = 5$ cm^{-1}) $\nu_2+\nu_4$ (1258 cm^{-1}, $V_e = 10.1$ cm^{-1}). Two other resonances, out of the range of Fig. 3, deserve to be mentioned: $\nu_1+\nu_4$ (1390 cm^{-1}, $V_e = 7.8$ cm^{-1}) and the ν_4 line (615 cm^{-1}, integrated cross section $A_4 = 6.60\ 10^{-2}\ A_3$).[15] The presence of $^{34}SF_6$ is clearly seen around 931 cm^{-1} and must be subtracted to obtain the $^{32}SF_6$ spectrum. Except for the preceding clearly identified resonances, no significant absorption can be seen. Only a very small absorption $\sim 10^{-4}$ of the spectrum maximum can be guessed between 750–840 and 1010–1150 cm^{-1}. Several IR inactive combinations must be mentioned: the ν_1 mode (775 cm^{-1}) or the ν_2 mode, out of the figure range (643 cm^{-1}). Other inactive combinations are also indicated with parentheses. Spectroscopic data about SF_6 can be found in Ref. 16.

The fluorescence spectra have been obtained at 0.388 Torr for the three fluences $\phi = 0.46$, 1.00, 1.86 J/cm^2 corresponding to the average energy absorbed $\langle\Delta E\rangle = 5000$, 11 500, 17 000 cm^{-1}. The corrected oscillator strength $dF_c/d\nu$, at the delay $+6$ μs is represented in Figs. 4(a), 4(b), and 4(c) for these respective energies. Several scales, X1, X10, X100, are used, according to the intensity. The computed contribution of $^{34}SF_6$ is represented, just as the spectrum C_0 corresponding to the pure ν_3 mode, reduced to a single Dirac peak at $\nu_3(E_v)$ ($\gamma = 0$). The difference between the experimental spectrum and C_0 represents the out-of-res-

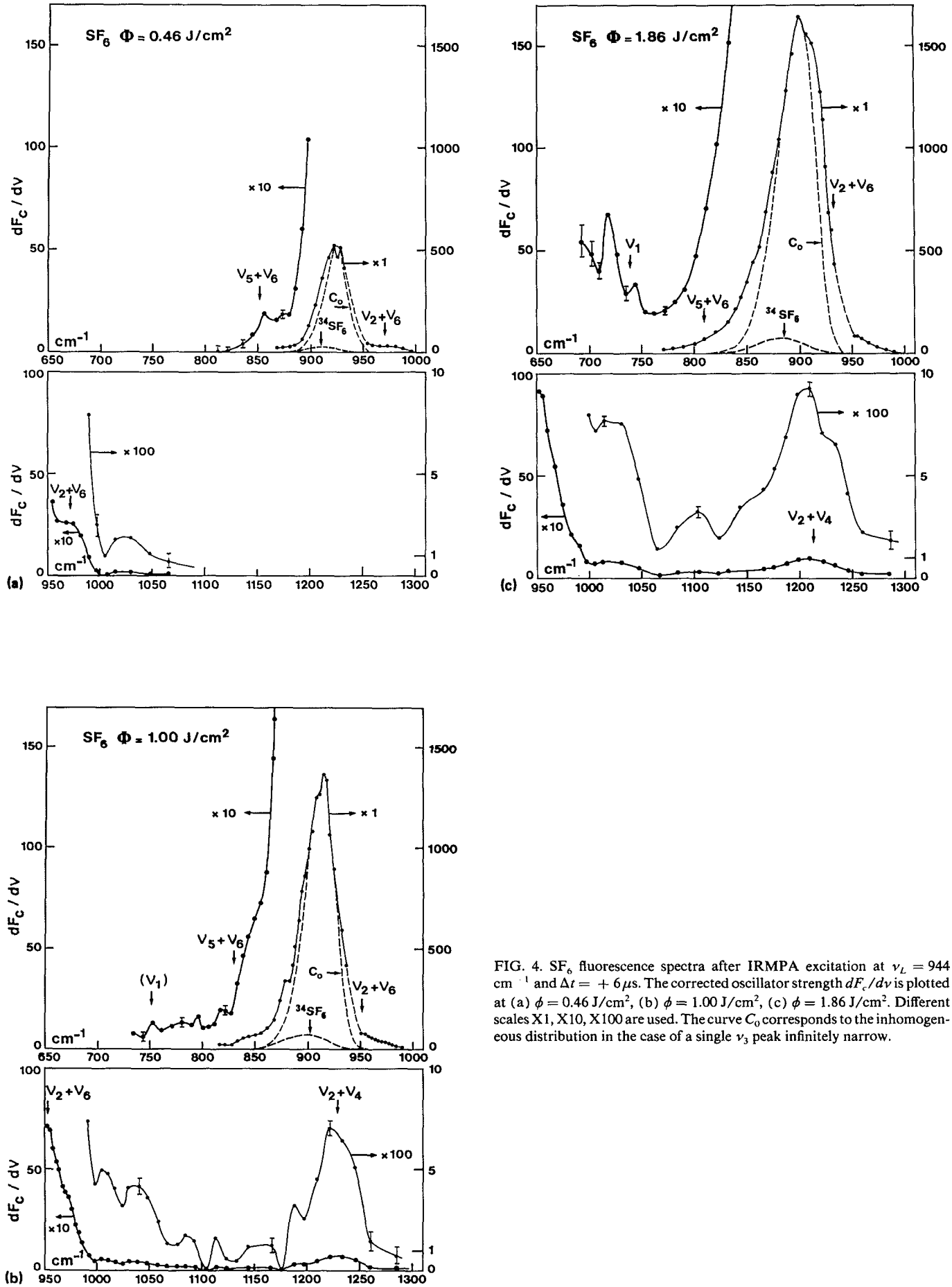

FIG. 4. SF_6 fluorescence spectra after IRMPA excitation at $\nu_L = 944$ cm^{-1} and $\Delta t = +6\,\mu s$. The corrected oscillator strength dF_c/dv is plotted at (a) $\phi = 0.46\,J/cm^2$, (b) $\phi = 1.00\,J/cm^2$, (c) $\phi = 1.86\,J/cm^2$. Different scales X1, X10, X100 are used. The curve C_0 corresponds to the inhomogeneous distribution in the case of a single ν_3 peak infinitely narrow.

onance redistributed oscillator strength, related to the $I_1(\nu)$ expression [Eq. (9)]. The Fermi resonances identified in the cold gas absorption spectrum are also indicated. Only a limited range has been explored at 0.46 J/cm^2, but a significant oscillator strength, $\sim 2.10^{-3}$ of the maximum, appears in the range 1000–1070 cm^{-1}, while in the cold gas absorption spectrum, the signal does not exceed 10^{-4} of the maximum. The appearance of an out-of-resonance oscillator strength becomes much more visible at 1.00 and 1.86 J/cm^2, where a significant signal is seen continuously from 650 to 1300

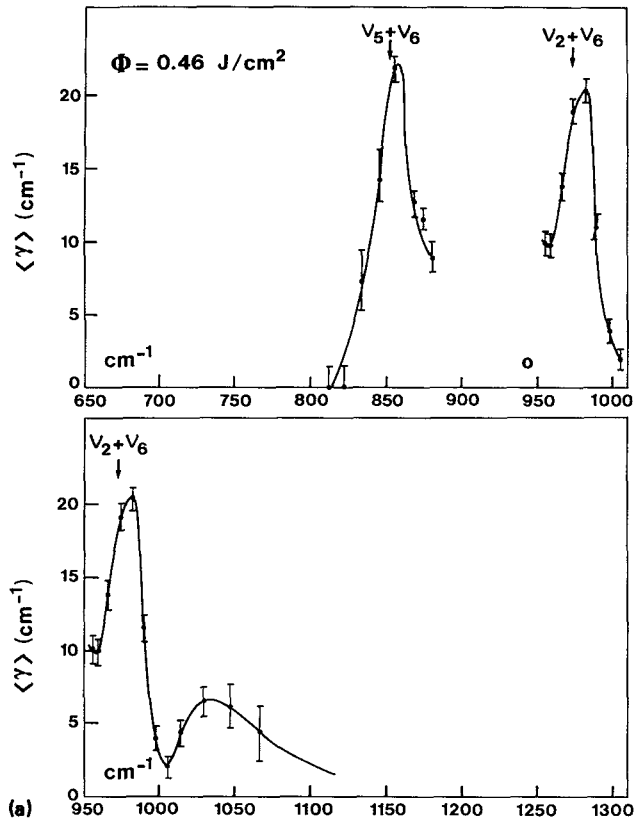

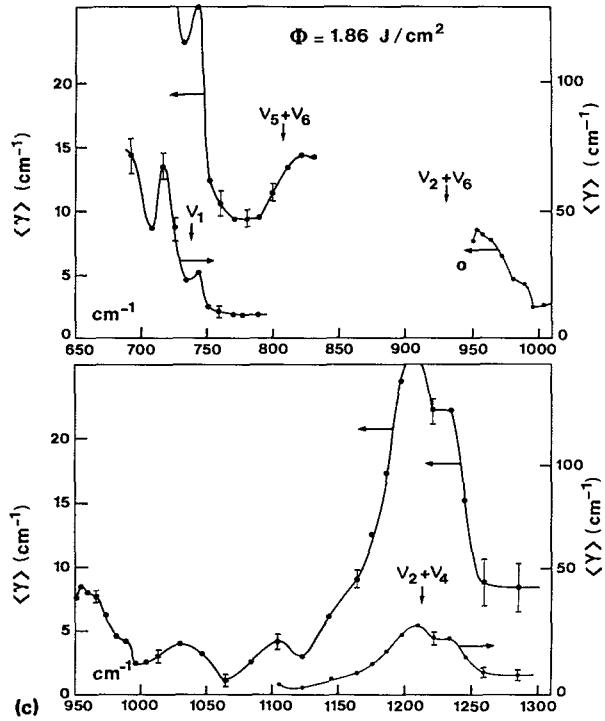

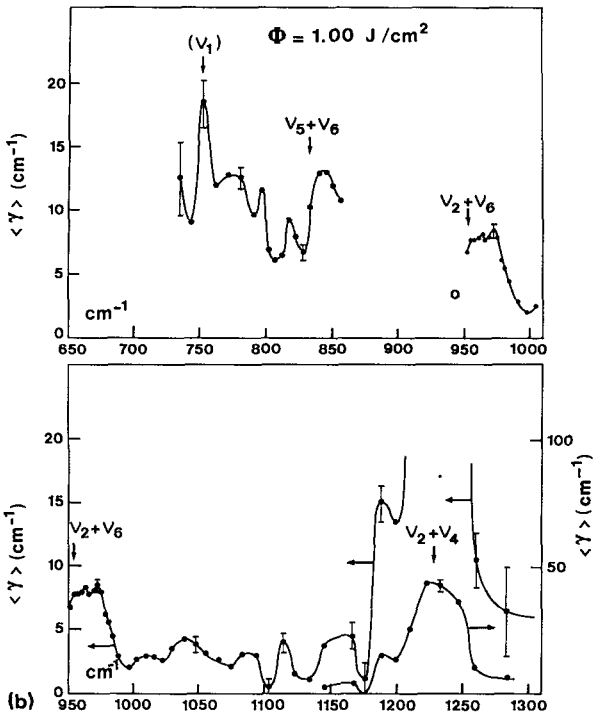

FIG. 5. Quasi-Lorentzian parameter $\langle\gamma(\nu)\rangle$ extracted from the SF_6 fluorescence data of the Fig. 4. (a) 0.46 J/cm^2, (b) 1.00 J/cm^2, (c) 1.86 J/cm^2.

cm^{-1}. Moreover, a new resonance appears in the range 700–750 cm^{-1} at 1.00 J/cm^2 and becomes very intense at 1.86 J/cm^2. The value corresponds approximately to the anharmonically shifted ν_1 mode, this one being, however, IR inactive in the discrete levels. We will call this new resonance the "(ν_1) cluster."

The quasi-Lorentzian parameter $\langle\gamma(\nu)\rangle$, deduced from $dF_c/d\nu$ using the procedure of Appendix B, has been plotted in Figs. 5(a), 5(b), and 5(c) for 0.46, 1.00, 1.86 J/cm^2. At 1.00 and 1.86 J/cm^2, two different scales are used, according to the values obtained. The different resonances $\nu_5+\nu_6$, $\nu_2+\nu_6$, and $\nu_2+\nu_4$ and the (ν_1) cluster are much more clearly apparent. There remains, in fact, a single large range free from intense isolated resonance between 1000 and 1150 cm^{-1}. In this range, $\langle\gamma\rangle$ exhibits, however, fluctuations from 1 to 5 cm^{-1} without strong variations vs the energy absorbed. At 1.00 J/cm^2, $\langle\gamma\rangle$ reaches a minimum value $\sim(0.5\text{–}1)\pm1$ cm^{-1} at two frequencies 1000 and 1175 cm^{-1} so that zero is inside the error bar. For $\nu<\nu_3$, there is only a small range, 800–830 cm^{-1} at 1.00 J/cm^2 and 760–800 cm^{-1} at 1.86 J/cm^2, which is not too much perturbed by the nearest resonances, and there, $\langle\gamma\rangle\sim10$ cm^{-1}. For $\nu>\nu_3$ there appears at the extreme part of the explored frequencies, between 1260–1280 cm^{-1}, another narrow range not dominated by $\nu_2+\nu_4$ and $\nu_1+\nu_4$ (not visible on the spectrum). There, $\langle\gamma\rangle$ is again about 6–8 cm^{-1}. At $\nu=944$ cm^{-1}, we have indicated by a circle the value of γ obtained from the IRMPA data.[4] It can be noticed that the result is comparable to that obtained in the present work in the range 1000–1150 cm^{-1}, free from secondary resonances.

As indicated in Sec. II and Appendix B, the secondary resonances α need a particular treatment, since it is the integrated value $\int d\nu\langle\Delta\gamma_\alpha\rangle\Delta\nu^2$ which gives the effective coupling $\langle|V_{e\alpha}|^2\rangle$. The result has been plotted in Fig. 6 for the resonances: $\nu_2+\nu_6$, $\nu_5+\nu_6$, $\nu_2+\nu_4$, and the (ν_1) cluster.

The value at $\langle E_v\rangle=1000$ cm^{-1} is that of the cold gas absorption spectrum. The behavior of these resonances is very different: The $\nu_2+\nu_6$ and the $\nu_5+\nu_6$ increase very slowly vs the energy, while the $\nu_2+\nu_4$ and the (ν_1) cluster have a much stronger variation. Although only two energies have been studied, it seems that the (ν_1) cluster appears at an energy threshold ~8000 cm^{-1}. It deserves to be mentioned that the spectra in Figs. 5(a), 5(b), and 5(c) allow us to extract an approximate value of the anharmonic constants a_s and a_α of the ν_3 mode and secondary resonances. It is interesting to compare the experimental anharmonic shift to the value predicted by the usual quadratic intramode and intermode anharmonicities X_{ij} known in the low energy levels.[16] It can be shown, as will be detailed in the subsequent paper, that the coefficient a_i of a mode i [Eq. (4e)] is related to the X_{ij}'s by

$$a_i=-\frac{1}{s}\left[\frac{2X_{ii}}{\nu_i(0)}g_i+\sum_{j\neq i}\frac{X_{ij}}{\nu_j(0)}g_j\right]. \tag{12a}$$

Here, g_i is the degeneracy of the mode i. For a Fermi resonance $\alpha=i+j$,

$$a_\alpha=a_i+a_j. \tag{12b}$$

The formulas (4e) and (12) can be refined but give the anharmonicity shift with an accuracy $\sim$5–10%. The positions of the different peaks, predicted by these formula have been indicated on the different spectra by an arrow (Figs. 4 and 5). The striking feature is the very good agreement between this prediction and the observed resonance peaks, even at $\langle E_v\rangle=17\,000$ cm^{-1}.

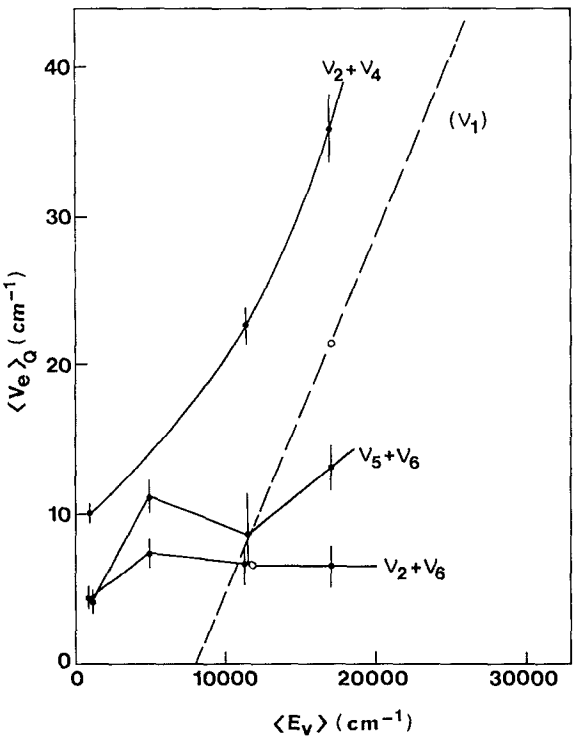

FIG. 6. Effective coupling $\langle V_e\rangle_Q=\langle|V_e|^2\rangle^{1/2}$ for the different secondary resonances of the SF_6 spectrum, vs the average vibrational energy $\langle E_v\rangle$.

The presence of secondary resonances raises the problem of their contribution far from their maximum, due to the Lorentzian wings. With an estimated parameter $\gamma_\alpha=5$ cm^{-1} for each of the secondary resonance, the contribution to $\langle\gamma\rangle$ is less than 10% everywhere, except in the following ranges: at 1.00 J/cm^2, around 1260 cm^{-1}, $\langle\gamma\rangle$ is diminished from 6.5 to 5.3 cm^{-1}; at 1.86 J/cm^2, around 770 cm^{-1}, $\langle\gamma\rangle$ is diminished from 9.5 to 7.0 cm^{-1}, and around 1260 cm^{-1} from 8.6 to 5.2 cm^{-1}. In the range 1000–1150 cm^{-1}, no correction is necessary.

Although this is not the main purpose of this work, collisional $V\rightarrow T,R$ data can be extracted from the fluorescence spectra observed vs time from 6 to 300 μs. These results are important for the analysis of an isotopic energy transfer effect reported elsewhere[12,17,18] and in future publications. As mentioned previously, the transfer between 6 to 15 μs is free from adiabatic expansion and the average vibrational energy lost by collision, $\langle\delta e_v\rangle$, can be deduced. The notion of collisional rate Z_0 is fairly conventional so that we have used the standard reference 10^7 s^{-1} $Torr^{-1}$ at the temperature 295 K, close to the hard-sphere value. The integrated oscillator strength

$$\Sigma_c(t)=\int d\nu\frac{dF_c}{d\nu}(t)$$

TABLE I. Collisional $V \rightarrow T,R$ energy transfer (in cm^{-1} per collision, using the conventional rate Z_0).

$\langle E_v(t_1)\rangle$ (cm^{-1})	$\langle \delta e_v(t_1)\rangle$ (cm^{-1})
11 500	− 22
17 000	− 39

is proportional to $\langle \bar{v}_3 \rangle$. The curve $\Sigma_c(t)/\Sigma_c(t_1)$ for $t_1 = 6\,\mu s$ allows to deduce $\langle \bar{v}_3(t)\rangle$ and then $T_v(t)$ and $\langle E_v(t)\rangle$, knowing the value $\langle E_v(t_1)\rangle$. $\langle \delta e_v(t_1)\rangle$ is immediately derived. The result is reported in Table I. This leads to an approximate dependence $\langle \delta e_v \rangle \propto E_v^{1.5}$.

B. Preliminary results for CF_3I

The results reported in this paragraph have been obtained in photosensitized experiments in which SF_6 is excited at $\nu_L = 944\ cm^{-1}$ in mixtures $SF_6/^{12}CF_3I$ or $SF_6/^{13}CF_3I$ (ratio 2/1). Then CF_3I is subsequently excited by collisional V–V transfer from SF_6 so that a thermal distribution is reached at $+300\,\mu s$. The conditions are therefore different from the previous one concerning pure SF_6 gas. First, the SF_6 spectrum must be subtracted. Second, an adiabatic expansion occurs,with a diffusion mixing between the hot and the cold zone. Then, corrected density and optical path n_1, l_1 must be used, and these effects must be taken into account to compute the vibrational temperature at $300\,\mu s$ and the average vibrational energy $\langle E_v^X \rangle$, where X means CF_3I. The entire procedure has been detailed in Ref. 12 and all the data will be published subsequently in relation with the isotopic energy transfer effect. Here, we want only to extract useful spectroscopic data about CF_3I at an average vibrational energy $\langle E_v^X \rangle \sim 3200\ cm^{-1}$.

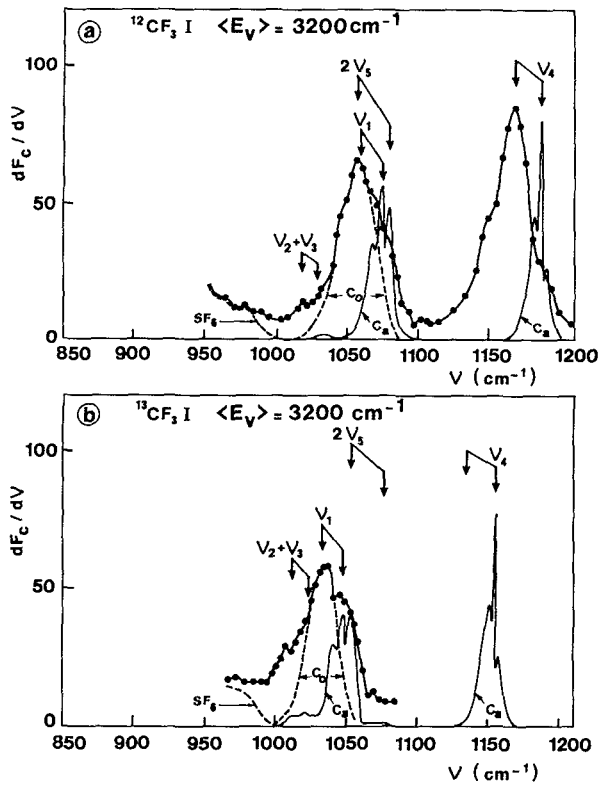

FIG. 7. CF_3I fluorescence spectrum at $\langle E_v^X \rangle = 3200\ cm^{-1}$ in a mixture SF_6/CF_3I, 2/1, $P = 0.580$ Torr. SF_6 is excited at $\nu_L = 944\ cm^{-1}$, $\phi = 1.00\ J/cm^2$, and $\Delta t = +300\,\mu s$. C_0 is the spectrum due to the inhomogeneous distribution in the case of a single ν_1 peak infinitely narrow. C_a is the low intensity absorption spectrum of the cold gas. (a) $^{12}CF_3I$, (b) $^{13}CF_3I$.

TABLE II. Effective couplings of CF_3I Fermi resonances.

	V_e (cm^{-1})	
Resonance	$E_v = 1000\ cm^{-1}$	$\langle E_v \rangle = 3200\ cm^{-1}$
$\nu_2 + \nu_3$	8.7 (12) 9.6 (13) 8.2 (F)	16.0 (12) 16.8 (13)
$2\nu_5$	3.1 (13) 2.6 (B)	12.7 (13)
$4\nu_6$	~2 (13) 0.94 (B)	

In the experiment reported here, the total pressure is 0.580 Torr and the fluence $\phi = 1.00\ J/cm^2$ which gives $\langle E_v^X \rangle = 3200\ cm^{-1}$ for CF_3I and $\langle E_v^A \rangle = 5500\ cm^{-1}$ for SF_6, at $t = +300\,\mu s$. Then, CF_3I is weakly excited in its QC according to the threshold value deduced in Ref. 19: $E_{QC} \simeq 6000\ cm^{-1}$. The resulting spectra are plotted in Figs. 7(a) and 7(b) for $^{12}CF_3I$ and $^{13}CF_3I$, respectively. For $^{12}CF_3I$, all the spectral range 900–1200 cm^{-1} has been explored, which allows one to see the two peaks ν_1 and ν_4. The SF_6 contribution is shown for $\nu < 1000\ cm^{-1}$. The absorption spectrum of the cold gas is indicated (curve C_a). The curve C_0 corresponds to a single peak ν_1 inhomogeneously broaden, but with infinitely narrow homogeneous width ($\gamma = 0$). The difference between the observed spectrum and C_0, after subtraction of the SF_6 spectrum, gives $2\nu_5$ and $\nu_2 + \nu_3$ Fermi resonances. It can be noticed that the oscillator strength is nonzero in all the range between the ν_1 and ν_4 peaks which indicates the presence of some other weak secondary resonances near 1100–1120 cm^{-1}.

The effective coupling $|V_e|$ of the two Fermi resonances can be deduced for the two isotopes in the case of the $\nu_2 + \nu_3$ and for the isotope 13 for the $2\nu_5$. The values are reported in the Table II and compared with the absorption data at the laboratory temperature ($E_v = 1000\ cm^{-1}$) extracted from our spectra or reported by Fuss[20] or Burger *et al.*[21] (indicated, respectively, by *F* and *B*).

A second piece of useful information is the anharmonic constant a_α of the different peaks (Table III). The value is deduced from the experimental data, either for the 12 or 13 isotope, and compared with the values computed by the formula (12) using the X_{ij} coefficients obtained by Fuss from absorption data.[20] The value $\nu_\alpha(0)$ is also indicated.

The values deduced from $^{12}CF_3I$ and $^{13}CF_3I$ differ because the $\nu_2 + \nu_3/\nu_1$ interaction becomes very strong for $^{13}CF_3I$, and the $2\nu_5/\nu_1$ interaction for $^{12}CF_3I$, so that formula (B5a) is no more accurate. The important point is that the

TABLE III. Anharmonic constants of CF_3I.

Line	$\langle E_v\rangle = 3200\ cm^{-1}$ a_α (unit 10^{-3})	$\langle F\rangle$ a_α	$\nu_\alpha(0)$ (cm^{-1}) $^{12}CF_3I$	$^{13}CF_3I$
ν_1	−5.7 (12) / −3.9 (13)	−5.2	1075.2	1047.6
$\nu_2+\nu_3$	−3.7 (12) / −4.9 (13)	−3.8	1030	1023
$2\nu_5$	−7.3 (13)	−8.0	1080	1077
ν_4	−6.7 (12)	−6.5	1187.5	1154.3
$4\nu_6$	⋯	−3.6	1046	1044

values obtained by Fuss are confirmed within 10%, when applied to a statistical distribution of the energy among the modes (the distribution is thermal in our case).

IV. DISCUSSION

Here, we want only to point out the striking conclusion deduced from our spectra. A detailed analysis and comparison with previously published work will be made in paper II of this series while a general theoretical framework suited for the description of QC molecular states will be developed in papers III and IV.

(1) From the cold gas absorption spectrum, it could be expected that two large ranges, 650–800 cm^{-1} and 1000–1150 cm^{-1} would be free from secondary resonances, so that the parameter $\langle\gamma\rangle$ would be characteristic of the local $\pi\rho|V_e|^2$ parameter. In fact, only the second of these ranges is relevant for this purpose because an unexpected line multiplet appears around 750 cm^{-1}. The link between this resonance and the ν_1 mode is an open question and could be a coincidence between the two frequencies, but we think that there exists a natural explanation for the appearance of an IR activity of the ν_1 mode in highly excited states. While the ν_1 mode is IR inactive for low energy levels, if we accept a separable modes approximation defining states $|v_1,...,v_s\rangle$, the best separable coordinates can be defined self-consistently, so that the best ν_1 mode around quantum numbers $v_2,...,v_s$ is different from the ν_1 mode around $v_2=\cdots=v_s=0$, corresponding to a rotation in the coordinate space. If a particular $v_2,...,v_s$ set corresponds to a nonspherical distortion of the molecule, an IR activity appears. In fact, due to IVR, the true eigenstate is a statistical superposition of $|v_1,...,v_s\rangle$ states around the given energy E_v and the IR oscillator strength of the ν_1 resonance is also an average over this statistical superposition which can be represented by the effective coupling $|V_e|$. As the IR activity is highly sensitive to the $v_2,...,v_s$ repartition, just as the ν_1 resonance frequency value, we can expect a fairly large spreading of the IR cluster, and the appearance of several peaks, as is observed in Figs. 5(b) and 5(c). This mechanism can be responsible in a more general way for modifications of the total integrated oscillator strength of all the resonances, according to their sensitivity to the intramode energy distribution. V_e can be interpreted as coming from a bilinear term $x_1x_3U_e(v_2,...,v_s)$ with U_e dispersed around 0 according to the (v_j) distribution. We must note that although $\langle U_e\rangle=0$ the oscillator strength is proportional to $\langle|U_e|^2$ and therefore nonzero.

(2) The effective couplings $|V_e|$ exhibit different variations vs the energy E_v (Fig. 6). Although the number of points is very limited, we can try an extrapolation of $|V_e|$ up to the dissociation threshold $E_d=32\,000\ cm^{-1}$, giving roughly: 7 cm^{-1} for $\nu_2+\nu_5$, 15 cm^{-1} for $\nu_5+\nu_6$, 60 cm^{-1} for the (ν_1) cluster, and 80 cm^{-1} for $\nu_2+\nu_4$. One general remark commands attention: Whatever the resonance α and the energy E_v, the criterion for a perturbative treatment is checked,

$$|V_{e\alpha}|<h\Delta\nu_\alpha, \tag{13}$$

where $h\Delta\nu_\alpha$ is the energy detuning from ν_3.

Thus the strongest couplings have a density too low to produce a dissipative redistribution, and they produce only perturbative secondary resonances or, in the case of the (ν_1) cluster, a modification of the IR activity.

(3) The positions of all the SF_6 resonances, up to $E_v=17\,000\ cm^{-1}$ appear very well predicted by the anharmonic shift $-a_\alpha E_v$, where a_α can be computed from the anharmonic quadratic coefficients X_{ij} of the low energy levels. The anharmonic shift is predicted with an error less than 10%. In the case of CF_3I this property has been checked only at $\langle E_v\rangle=3200\ cm^{-1}$, i.e., below the QC threshold ($\sim$6000 cm^{-1}) but the experimental conditions ensure a statistical distribution of the mode energies. Thus the low energy X_{ij} coefficients can be used as a useful guide to guess the positions of the different resonances up to the dissociation energy. We will use this approach for CF_3I in the subsequent paper.

(4) The value of $\langle\gamma\rangle$ obtained in the single large range free from strong secondary resonances is typically around 2–4 cm^{-1}. It should be mentioned that in the two other narrow ranges, not too much perturbed by resonances, around 800 and 1280 cm^{-1}, $\langle\gamma\rangle$ is again of the same magnitude 5–7 cm^{-1}, after correction of the adjacent resonance contributions. A very interesting fact is the comparison with the γ parameter obtained from IRMPA data at $\nu_L=944\ cm^{-1}$ in Ref. 4 and indicated by a circle in Fig. 5. The experimental conditions are very different: low intensity monophoton spontaneous emission in the IR fluorescence measurements reported in this work, high intensity (MW/cm^2) multiphoton absorption and induced emission in the IRMPA data analyzed in Ref. 4. Nevertheless, the γ parameter obtained in this last case is in very good agreement with IR fluorescence data: 3 cm^{-1} for $\langle E_v\rangle\sim11\,500\ cm^{-1}$, 5 cm^{-1} for $\langle E_v\rangle\sim17\,000\ cm^{-1}$. This gives high confidence to the validity of the obtained parameter γ for the quasi-Lorentzian representation of the oscillator strength redistribution. It is also interesting to observe that the variation of $\langle\gamma\rangle$ from 11 500 to 17 000 cm^{-1}, in the range 1000–1150 cm^{-1} is weak.

(5) However, the value of $\langle\gamma\rangle$ must be analyzed with caution for two reasons. First, $\langle\gamma\rangle$ is an average over an inhomogeneous distribution P_v corresponding to a width $a_3 2\Delta_v\sim35\ cm^{-1}$ at 1.00 J/cm^2 and 45 cm^{-1} at 1.86 J/cm^2. Then, all structures at a smaller scale are spread out and not visible. So, we must always keep in mind that a flat $\langle\gamma\rangle$ distribution can also be interpreted as due to resonances α with

an effective coupling $|V_{e\alpha}|$ and a spacing ϵ such that

$$\pi \frac{|V_{e\alpha}|^2}{\epsilon} = \langle \gamma \rangle, \tag{14a}$$

$$\epsilon \lesssim a_3 2\Delta_v. \tag{14b}$$

Then, the interpretation is ambiguous. Second, and more decisively, we observe in Figs. 5(b) and 5(c) clear variations of $\langle \gamma \rangle$ with a spacing $\simeq a_3 2\Delta_v$ between the successive maxima. This is the indication that the major part of the observed $\langle \gamma \rangle$ is in fact related to weak secondary resonances with such a spacing ~ 30 cm^{-1}. With $\langle \gamma \rangle \sim 3$ cm^{-1} and $\epsilon = 30$ cm^{-1}, we get $|V_{e\alpha}| \sim 5$ cm^{-1}.

Thus we are guided to a description of the oscillator strength distribution very different from that of a model assuming a flat distribution of the $|V_{ij}|^2$ matrix elements. Apart from the well defined Fermi resonances known at low energies, there exists a new strong resonance—the (ν_1) cluster—but also a series of medium intensity secondary resonances characterized by $|V_{e\alpha}| \sim 5$ cm^{-1} and $\epsilon \sim 30$ cm^{-1}. We can observe that this new set of resonances checked the perturbative redistribution condition of the BJ model:

$$\pi |V_{e\alpha}| < \epsilon, \tag{15}$$

i.e., once again, these resonances are not able to ensure a dissipative redistribution of the ν_3 energy content.

Then one question arises: What is the oscillator strength part responsible for the dissipative redistribution which can be represented by a flat function γ_d? From the minima of $\langle \gamma \rangle$ observed in our spectra, we can only state that this part verifies

$$\gamma_d \lesssim 1\text{–}1.5 \text{ cm}^{-1}, \tag{16}$$

but in fact, we are not able to state from our data that γ_d is not very small or even strictly zero. Only the observation of intermode randomization after IRMPA in several experiments,[19] on a ns scale, ensures that $\gamma_d > 10^{-3}$ cm^{-1} (Eq. 1). Although our data $\langle \gamma \rangle$ give a quantitative constraint to the oscillator strength repartition there remains an important uncertainty about the IVR scheme at frequency scales $\lesssim a_3 \Delta_v$ and about the value of the γ_d parameter representing the dissipative part within the limit (16).

V. CONCLUSION

The out-of-resonance fluorescence method has proven its efficiency to obtain important information about the intramolecular redistribution process. A fairly unexpected scheme arises: In the spirit of the "restricted exchange theory" (RQE) of Stone *et al.*,[22,23] a hierarchy of couplings of decreasing intensity and increasing effective density of states appears. In the first order the Fermi resonances are found but also a new resonance, probably due to the ν_1 mode, slightly rotated in the space of normal coordinates. Then, the effective couplings V_e and the typical spacing ϵ are $V_e \sim 20$ cm^{-1}, $\epsilon \sim 170$ cm^{-1}. In the second order, a set of resonances is visible, with $V_e \sim 5$ cm^{-1} and $\epsilon \sim 30$ cm^{-1}. The striking fact is that these most intense couplings are only able to produce a perturbative redistribution of the ν_3 oscillator strength. The dissipative redistribution can only be achieved by couplings with smaller intensity and higher effective density of states and could be represented by a parameter γ_d not exceeding 1–1.5 cm^{-1}. The inhomogeneous spreading does not allow us to extract more definite information but the comparison with other data, such as IRMPA cross sections or picosecond experiments can remove this indefiniteness. This will be attempted in the subsequent paper. From an experimental point of view, it would be useful to get spectra for a greater number of energy values, mainly around the QC threshold, near 4000 cm^{-1} for SF_6. The observation of the (ν_1) cluster at $\nu < 700$ cm^{-1} should also be interesting.

APPENDIX A: RELATION BETWEEN $dF_e/d\nu$ AND $dF_c/d\nu$

The optical path of the emitted oscillator strength can be considered as a succession of transmission and absorption paths through homogeneous media, at temperature T_1 (irradiated zone) or T_0 (cold zone). The molecular density is n_0 whatever the zone because at $t = +6\,\mu$s, no gas expansion has occurred. For longer times, a correction is necessary due to this expansion. The lengths of the two zones are, respectively, l_1 and l_0. The equation for the intensity $J(\nu) = dI/d\nu$ inside each homogeneous medium is, along the distance x,

$$\frac{dJ}{dx} = -n_0 \sigma_a J + n_0 J_c, \tag{A1}$$

where $\sigma_a(\nu,T)$ is the absorption cross section and $J_c(\nu,T)$ (W/Hz×Ster) is the fluorescence probability emitted by one molecule.

The Einstein relation between the blackbody emission $B(\nu,T)$ (W/Hz×cm^2×Ster), σ_a and J_c is

$$B\,\sigma_a = J_c = \nu^3\, dF_c/d\nu \tag{A2}$$

with

$$B(\nu) = C_B \frac{\nu^3}{\exp(h\nu/kT) - 1}. \tag{A3}$$

(A1) and (A2) give

$$J(x) - B = [J(0) - B]\, e^{-n_0 \sigma_a x}. \tag{A4}$$

At the reflection on the mirrors, an attenuation $e^{-\theta}$ is introduced, due to the geometrical distortions. Then, from one zone to the other, there is a relation

$$J_{n+1} = aJ_n + b,$$

which can be rewritten

$$(J_{n+1} - \beta) = a(J_n - \beta)$$

with $\beta = b/(1-a)$.

Grouping the paths along one cold zone and one hot zone, the solution J_e at the cell exit, after K elementary paths, can be expressed by

$$J_e - \beta = a^k (B_1 - \beta), \tag{A5a}$$

with

$$a = a_0 a_1, \tag{A5b}$$

$$\beta = B_1 \frac{(1-a_1)a_0}{1-a} + B_0 \frac{1-a_0}{1-a}, \tag{A5c}$$

$$a_0 = e^{-n_0 \sigma_{a_0} l_0 - \theta}, \tag{A5d}$$

$$a_1 = e^{-n_1 \sigma_{a1} l_1}. \tag{A5e}$$

The detector is sensitive to the signal difference $J_e - B_0$, so that using (A5a), we get finally for a collected surface $\delta\Sigma$ and a solid angle $\delta\Omega$

$$S(\nu) = \delta\Sigma\,\delta\Omega C_f(\nu)(B_1 - B_0)(1 - a_1)a_0 \frac{1 - a^k}{1 - a}. \tag{A6}$$

This formula allows, in principle, the extraction of a_1 from S, and then the knowledge of $\sigma_{a1}(\nu)$, J_{c1}, or $dF_c/d\nu$, but there is one difficulty due to the absolute calibration between $J_e - B_0$ and $S(\nu)$. There are strong uncertainties about $\delta\Sigma$, $\delta\Omega$, and $C_f(\nu)$, so that (A6) must be used for relative values. To solve this problem, we can consider oscillator strengths relative to the maximum of the spectrum at ν_m

$$X(\nu) = \frac{dF_c}{d\nu}(\nu) \Big/ \frac{dF_c}{d\nu}(\nu_m). \tag{A7a}$$

There remains one unknown parameter,

$$\frac{dF_c}{d\nu}(\nu_m) = f_m, \tag{A7b}$$

which can be self-consistently determined from the integrated cross section

$$A = \int \frac{d\nu}{c}\,\sigma_a(\nu) \tag{A8}$$

using the Eqs. (A2) and (A3).

For a given mode, A is independent on the vibrational energy in the mode and is therefore known from the low intensity absorption spectroscopy. For example, $A_3 = 1.765\ 10^{-16}$ cm for the ν_3 SF_6 mode.[15]

Practically, the determination of $X(\nu)$ and f_m can be obtained as follows. $e^{-\theta}$ is measured using the experimental amplification of the system of mirrors for the empty cell

$$G = \frac{1 - e^{-k\theta}}{1 - e^{-\theta}}.$$

$G = 6.5$, and $k = 10$ (Fig. 2).

$n_0 = n_1$ is computed taking into account the dissociation up to the laser pulse N. The absorption in the cold zone, $\sigma_{a0}(\nu)$, can be obtained from the IR spectrometer and the normalization (A8), but in this experiment, σ_{a0} is negligible out of the blind zone of the absorbing cell C_a. In the presence of another gas, the correction $n_0\sigma_{a0}l_0$ should be necessary, but for pure SF_6, this is not the case.

We can notice that if the reabsorption in the irradiated zone was very strong ($a_1 \to 0$), $S(\nu)$ should be proportional to the blackbody emission difference $B_1 - B_0$, as it must be the case. To have an observable effect, we must be in the condition $\epsilon_1 = n_1\sigma_{a1}l_1 \ll 1$ and then $1 - a_1 \sim n_1\sigma_{a1}l_1a_1^{1/2}$. Obviously, the same expansion for a_1^k is not justified, since $k = 10$. Using (A2), we get

$$X(\nu) = X_0(\nu)\frac{K(\nu_m)}{K(\nu)}, \tag{A9a}$$

with

$$X_0(\nu) = \frac{S(\nu)}{S(\nu_m)}\,\frac{H(\nu_m)}{H(\nu)}, \tag{A9b}$$

$$H(\nu) = C_f(\nu)\left[1 - \frac{B_0(\nu)}{B_1(\nu)}\right]\nu^3 a_0^{1/2}, \tag{A9c}$$

$$K(\nu) = a^{1/2}\,\frac{1 - a^k}{1 - a}. \tag{A9d}$$

Obviously, $X(\nu_m) = X_0(\nu_m) = 1$.

K is the factor giving the cell amplification, taking into account the reabsorption. It is a function of the single variable $\theta + n_0\theta_0\sigma_{a0} + n_1l_1\sigma_{a1}$ which depends on $X(\nu)$ through $\epsilon_1 = n_1l_1\sigma_{a1}$. ϵ_1 is unknown but can be expressed from (A2) and (A3),

$$\epsilon_1 = n_1l_1(e^{h\nu/kT} - 1)X(\nu)/\mu. \tag{A10a}$$

μ is a constant determined by (A8).

$$\mu = \frac{C_B}{f_m} = \frac{1}{A_3}\int d\,\frac{\nu}{c}(e^{h\nu/kT} - 1)X(\nu). \tag{A10b}$$

$X_0(\nu)$ can be considered as a zero order approximation of X, when K is chosen constant at the value $K(\nu_m)$. The difficulty in the previous set of equations is that K depends on the constant μ, which depends on X through an integral. It is convenient to start with the zero order approximation $X_0(\nu)$ and the corresponding μ_0 value. Then, $K(\nu)$ and μ can be expanded simultaneously vs $\Delta X = X - X_0$, giving relations of the form

$$\Delta X \sim a(\nu) - b(\nu)\Delta\mu, \tag{A11a}$$

$$\Delta\mu \sim I_a - I_b\Delta\mu, \tag{A11b}$$

where $\Delta\mu$ is expressed from (A10b) and

$$I_a = \int d\,\frac{\nu}{c}(e^{h\nu/kT} - 1)a(\nu) \tag{A11c}$$

(idem from I_b).

Then

$$\Delta\mu = I_a/(1 + I_b), \tag{A12a}$$

$$\Delta X = a - bI_a/(1 + I_b). \tag{A12b}$$

This gives the first order solution X_1, which is generally quite sufficient. If necessary, the procedure can be continued.

APPENDIX B: RELATION BETWEEN $dF_c/d\nu$ AND γ

1. Parameters of the function $L(E \to E')$

$$V_e(E \to E') = \frac{\langle s|V|E'\rangle}{\||s\rangle\|} = \frac{\langle E|dV|E'\rangle}{\|d|E\rangle\|}, \tag{B1a}$$

$$E_s = \frac{\langle s|H|s\rangle}{\||s\rangle\|^2} = \frac{\langle E|dVd|E\rangle}{\|d|E\rangle\|^2}, \tag{B1b}$$

$$F(E') = PP\frac{1}{\pi}\int dE''\,\frac{\gamma(E \to E'')}{E' - E''}. \tag{B1c}$$

PP is the principal part.

The shift $F(E')$ is at most of the same magnitude as γ and varies over the same scale. The role of rotations is simplified, assuming as for discrete levels, three P, Q, R transitions with an effective rotational constant B_e,

$$E_s - E = h\nu_s(E_v) + \epsilon_R 2B_eJ, \tag{B2}$$

with $\epsilon_R = 0, \pm 1$.

In all cases, for an optical frequency ν,

$$E' - E = h\nu. \tag{B3}$$

In the BJ model, in which the lines have a spacing ϵ not necessarily equal to the ultimate spacing, the denominator constant is

$$D^2 = \gamma^2 + V_e^2 = \gamma^2 + \frac{\epsilon\gamma}{\pi}. \tag{B4}$$

When $\epsilon \to 0$, the second term is negligible, but if the relaxation occurs through a restricted set of discrete lines, with a spacing of the same order as the inhomogeneous width, this second term is comparable to the first. Then, due to the inhomogeneous contribution, there is some uncertainty about the parameter D, but this is not very important out of resonance, where $\Delta\nu \gg D$ and the error, in $D^2/\Delta\nu^2$, is typically less than a few percents.

2. Treatment of a perturbative secondary resonance

If there exist isolated resonances α corresponding to states at energy E_α^- when the coupling $V_{e\alpha}(E_v)$ is omitted, we have at first order for perturbative resonances

$$P_\alpha = \frac{|V_{e\alpha}|^2}{(E_\alpha - E_s)^2 + |V_{e\alpha}|^2}, \tag{B5a}$$

with the energy position

$$E_\alpha = E_\alpha^- + \frac{|V_{e\alpha}|^2}{E_\alpha^- - E_s}. \tag{B5b}$$

These expressions show that the resonances α can be incorporated in the quasi-Lorentzian expression through a local peak $\Delta\gamma_\alpha$ in the numerator (Eq. 5 of the text) but with a limited variation of the denominator, since

$$F_\alpha = 0, \tag{B6a}$$

$$D_\alpha^2 = |V_{e\alpha}|^2. \tag{B6b}$$

It can be remarked that this regular behavior of the denominator is obtained only through a slight shift $E_\alpha^- \to E_\alpha$ of the peak in the numerator. This point will be developed in the papers III and IV.

In the previous expressions, $|V_{e\alpha}|^2$ and E_α^- have, in general, a dependence on E_v. The E_α^- dependence can be represented by an anharmonic shift,

$$E_\alpha^- - E_v = h\nu_\alpha(E_v) = h\nu_\alpha(0) - a_\alpha E_v, \tag{B7}$$

i.e., an expression similar to that of E_s [Eq. (4d) of the text, and if needed the rotations can be included by Eq. (B2)].

3. Extraction of $\langle\gamma\rangle$

The quasi-Lorentzian function L in Eq. (6b) of the text can be expressed as

$$L = \frac{1}{\pi}\frac{\gamma(E_v \to E_v + h\nu)}{[h\Delta\nu(E_v)]^2 + D^2} \tag{B8a}$$

with

$$\Delta\nu = \nu - \nu_s(E_v). \tag{B8b}$$

Rotations have been omitted here, for the sake of simplicity. As explained in the text, the integral I is separated in the two parts I_1 and I_2. I_2 is only a correction and the expression in the Eq. (10) of the text is sufficient. The improved evaluation of $I_1(\nu)$ can be made as follows. As a first approximation, D is neglected in Eq. (B8) compared to $h\Delta\nu = h\nu - h\nu_s(E_v)$, the correction being made as a perturbation. The denominator variation is represented around $\langle E_v\rangle$ as

$$e^{K_L(E_v - \langle E_v\rangle)}/[h\Delta\nu(\langle E_v\rangle)]^2$$

with $K_L = -2a_s/h\Delta\nu(\langle E_v\rangle)$. ($a_s$ is the anharmonicity of the $|s\rangle$ resonance.)

The normalized function

$$\bar{P}(E_v) = P(E_v)\bar{v}_3(E_v)/\langle\bar{v}_3\rangle$$

is represented by a Gaussian function

$$G(E_v) = \sqrt{\pi}K_p \exp[-K_p^2(E_v - \langle E_v\rangle - \delta_p)^2]$$

with $K_p \sim 1/\Delta_v$, and δ_p allows to fit the maximum.

Then, $I_1(\nu)$ has the following expression:

$$I_1(\nu) = \frac{1}{\pi}\frac{\langle\bar{v}_3\rangle_P \exp[K_L\delta_p + (K_L^2/4K_p^2)]}{[h\nu - h\nu_s(\langle E_v\rangle)]^2 + \langle D^2\rangle}\langle\gamma(\nu)\rangle_{\bar{Pd}}, \tag{B9}$$

where $\bar{P}d$ is the shifted function

$$\bar{P}d(E_v) = \bar{P}\left(E_v - \frac{K_L}{2K_p^2}\right).$$

The Gaussian modelization of $\bar{P}$ is only used to obtain the main effect of the denominator variation around $\langle E_v\rangle$: The average must be computed over a shifted distribution, and there appears a correcting factor in front of $\langle\gamma\rangle$. The parameter $\langle D^2\rangle$ can be obtained replacing γ by $\langle\gamma\rangle$ in (B4), assuming a given hypothesis for the spacing ϵ. The previous approximations are quite sufficient and does not introduce errors greater than a few percents in the worst cases.

4. Case of an isolated secondary resonance α

The resonance α is assumed to be perturbative and incorporated in L as indicated in Appendix B 2. $\Delta\gamma_\alpha(\nu)$ is given by Eq. (5) in the text, with $E' = E_v + h\nu$, so that the α contribution is

$$\Delta I_\alpha(\nu) = \bar{v}_3(E_v)\frac{1}{\pi}\frac{\pi|V_{e\alpha}(E_v)|^2}{(E_\alpha - E_s)^2 + |V_{e\alpha}(E_v)|^2}\frac{P_v(E_v)}{a_\alpha} \tag{B10a}$$

with E_v given by

$$h\nu = h\nu_\alpha(0) - a_\alpha E_v \tag{B10b}$$

and

$$E_\alpha - E_s = h\nu - h\nu_s(E_v). \tag{B10c}$$

Then, we obtain the remarkable result that the integration of the α peak gives $\langle|V_{e\alpha}(E_v)|^2\rangle_{\bar{Pd}}$ in the same way as $I(\nu)$ gives $\langle\gamma(\nu)\rangle_{\bar{Pd}}$, the procedure being described in Appendix B 3.

[1] N. R. Isenor and M. C. Richardson, Appl. Phys. Lett. **18**, 224 (1971).
[2] J. F. Bott, Appl. Phys. Lett. **32**, 624 (1978).
[3] M. Bixon and J. Jortner, J. Chem. Phys. **48**, 715 (1968).
[4] C. Angelié and Ph. Millié, Chem. Phys. **82**, 171 (1983).
[5] (a) H. S. Kwok and E. Yablonovitch, Phys. Rev. Lett. **41**, 745 (1978); (b) J. G. Black, P. Kolodner, M. J. Schultz, E. Yablonovitch, and N. Bloembergen, Phys. Rev. A **19**, 704 (1979); (c) H. S. Kwok, E. Yablonovitch, and N. Bloembergen, *ibid.* **23**, 3094 (1981); (d) R. C. Sharp, E. Yablonovitch, and N. Bloembergen, J. Chem. Phys. **74**, 5357 (1981); (e)

P. Mukherjee and H. S. Kwok, Chem. Phys. Lett. **111**, 33 (1984); (f) H. S. Kwok and P. Mukherjee, SPIE **742**, 25 (1987); (g) P. Mukherjee and H. S. Kwok, J. Chem. Phys. **87**, 128 (1987).
[6]C. Angelié and R. Capitini, Sixth Int. School Quant. El. Varna, 1990 (World Scientific, Singapore, 1990).
[7](a) V. N. Bagratashvili, S. I. Ionov, V. S. Letokhov, V. N. Lokhman, G. N. Makarov, and A. A. Stuchebrukhov, Sov. Phys. JETP **66**, 670 (1987); (b) S. I. Ionov, Spectrochim. Acta **43** A N° 2, 167 (1987); (c) S. I. Ionov and V. N. Bagratashvili, Chem. Phys. Lett. **146**, 596 (1988); (d) V. N. Bagratashvili, S. I. Ionov, A. A. Stuchebrukhov, V. S. Letokhov, V. N. Lokhman, and G. N. Makarov, *ibid.* **146**, 599 (1988); (e) S. I. Ionov, A. A. Stuchebrukhov, V. N. Bagratashvili, V. N. Lokhman, G. N. Makarov, and V. S. Letokhov, Appl. Phys. B **47**, 229 (1988).
[8](a) O. V. Boyarkin, S. I. Ionov, and V. N. Bagratashvili, Chem. Phys. Lett. **146**, 106 (1988); (b) S. I. Ionov and A. A. Kobakhidze, Appl. Phys. B **48**, 507 (1989).
[9]P. G. Smith and J. D. MacDonald, J. Chem. Phys. **92**, 1004 (1990).
[10]H. L. Welsh, J. Opt. Soc. Am. **45**, 338 (1955).
[11]S. S. Alimpiev, B. O. Zikrin, L. Holtz, S. M. Nikiforov, V. V. Smirnov, B. G. Sartakov, V. I. Fabelinski, and A. L. Shtarkov, JETP Lett. **38**, 421 (1983).
[12]C. Angelié, thesis (University Pierre et Marie Curie, Paris, 1990).
[13]U. Fano, Phys. Rev. **124**, 1866 (1961).
[14](a) B. Carmeli, I. Schek, A. Nitzan, and J. Jortner, J. Chem. Phys. **72**, 1928 (1980); (b) B. Carmeli and A. Nitzan, *ibid.* **72**, 2054 (1980); (c) B. Carmeli and A. Nitzan, *ibid.* **72**, 2070 (1980).
[15]D. S. Dunn, K. Scanlon, and J. Overend, Spectrochim. Acta **38A**, 841 (1982).
[16]R. S. MacDowell, B. J. Krohn, H. Flicker, and M. C. Vasquez, Spectrochim. Acta **42A**, 351 (1986); (b) R. S. MacDowell and B. J. Krohn, *ibid.* **42A**, 371 (1986).
[17]M. Cauchetier, M. Luce, and C. Angelié, Chem. Phys. Lett. **88**, 146 (1982).
[18]C. Angelié, M. Cauchetier, and J. Paris, Chem. Phys. **66**, 129 (1982).
[19](a) V. N. Bagratashvili, V. S. Doljikov, V. S. Letokhov, A. A. Makarov, L. J. Bagratashvili, V. S. Doljikov, V. S. Letokhov, A. A. Makarov, L. J. Maljavkin, E. A. Ryabov, E. G. Silkis, and Yu. G. Vainer, Opt. Commun. **38**, 31 (1981); (b) V. N. Bagratashvili, Yu. G. Vainer, V. S. Dolzhikov, S. F. Kol'yakov, V. S. Letokhov, A. A. Makarov, L. P. Maljavkin, E. A. Ryabov, E. G. Silkis, and V. D. Titov, Sov. Phys. JETP **53**, 512 (1981).
[20]W. Fuss, Spectrochim. Acta **38A**, 829 (1982).
[21]H. Bürger, K. Burczyk, H. Hollenstein, and M. Quack, Mol. Phys. **55**, 255 (1985).
[22]M. F. Goodman, J. Stone, and E. Thiele, "Multiple photon excitation and dissociation of polyatomic molecules" in *Topics in Current Physics*, edited by C. D. Cantrell (Springer-Verlag, Paris, 1986), Chap. 6.
[23]J. Stone, *Lasers, molecules, and methods*, Adv. Chem. Phys. **73** (Wiley, New York, 1989), Chap. 11.